PHYSICAL REVIEW B **68**, 060502(R) (2003)

Decoherence in a Josephson-junction qubit

A. J. Berkley,* H. Xu, M. A. Gubrud, R. C. Ramos, J. R. Anderson, C. J. Lobb, and F. C. Wellstood
Center for Superconductivity Research, Department of Physics, University of Maryland, College Park, Maryland 20742, USA
(Received 2 May 2003; published 18 August 2003)

The zero-voltage state of a Josephson junction biased with constant current consists of a set of metastable quantum energy levels. We probe the spacings of these levels by using microwaves to induce transitions and thereby enhance the escape rate to the voltage state. The widths of the resonances give a measurement of the spectroscopic coherence time of the two metastable states involved in the transitions. We observe a decoherence time shorter than that expected from dissipation alone in resonantly isolated 20×5 μm^2 area Al/AlOx/Al junctions at 60 mK. The data are well fit by a model that includes the dephasing effects of both low-frequency current noise and the escape rate to the voltage state. We discuss implications for quantum computation using current-biased Josephson-junction qubits, including limits on the minimum number of levels needed in the well.

DOI: 10.1103/PhysRevB.68.060502 PACS number(s): 03.67.Lx, 85.25.Cp, 03.65.Yz,78.70.Gq

Research in 1980s definitively showed that the phase difference across a single current-biased Josephson junction can behave quantum mechanically.[1,2] The recent proposal that an isolated current-biased Josephson junction could serve as a qubit[3] in a quantum computer has preceded a resurgence of interest in this simple system[4–8] that has included observations of Rabi oscillations as well as states of two coupled qubits.

Designing a quantum computer based on isolated Josephson junctions raises many issues. Isolation of the junction from its bias leads must be achieved by controlling the high-frequency electromagnetic environment that the junction couples to.[2] At the very least, this isolation must be effective around the resonant frequency of the junction. In addition, at lower frequencies, current noise will tend to cause decoherence in the junction state.[9] Also, during typical gate operations the junction will operate in a strongly anharmonic regime that is reached by applying a large bias current through the junction. For this high bias regime, however, there is an increased escape rate from the upper qubit state. In this paper, we describe how both the escape rate and the low-frequency current noise cause decoherence, and report results on measurements of these effects in Al/AlOx/Al Josephson junctions.

Consider a Josephson junction shunted by capacitance C, having a critical current I_0, and a parallel shunting impedance $R(\omega)$ due to the external wiring (see Fig. 1). The supercurrent I through the junction is given by the Josephson relation $I=I_0\sin(\gamma)$, and the voltage by $V=(\Phi_0/2\pi)d\gamma/dt$, where γ is the gauge-invariant phase difference between the superconducting wave functions on each side of the junction. For $I<I_0$, the phase γ may be trapped in a well of the Josephson washboard potential $U=-(\Phi_0/2\pi)I_0\cos\gamma-(\Phi_0/2\pi)I\gamma$ or it may be in a running state with a nonzero average dc voltage.[10]

Quantizing the single junction system in the absence of dissipation leads to metastable states that are localized in the wells (see Fig. 2) and adds the possibility of escape to the continuum running states by quantum tunneling from the ith level with a rate $\Gamma_{i\to\infty}$. The energy barrier $\Delta U=(I_0\Phi_0/\pi)[\sqrt{1-(I/I_0)^2}-(I/I_0)a\cos(I/I_0)]$ to the continuum decreases as the bias current is increased, leading to a rapid increase in the tunneling rate with bias current:[11]

$$\Gamma_{i\to\infty}=\omega_p\frac{(432N_s)^{i+1/2}}{(2\pi)^{1/2}i!}e^{-36N_s/5}, \tag{1}$$

where $\omega_p=\sqrt{(2\pi I_0)/(\Phi_0 C)}[1-(I/I_0)^2]^{1/4}$ is the classical oscillation frequency and $N_s=\Delta U/\hbar\omega_p$ is approximately the number of levels in the well. As the energy barrier is lowered, the energy levels of the states in the well move closer together and the well becomes more anharmonic until, at $I=I_0$, the energy barrier disappears.

The observed escape rate of the system from the zero-voltage state to the finite voltage state at a given bias point is $\Gamma=\Sigma_{i=0}^{n}\Gamma_{i\to\infty}P_i$, where P_i is the probability of the junction being in the ith state. An ac current I_{ac} (either external or thermally generated) can induce transitions between levels i and j in the well with a rate $\Gamma_{i\to j}\propto|(\Phi_0/2\pi)I_{ac}\langle i|\gamma|j\rangle|^2$. Since $\Gamma_{1\to\infty}\simeq 500\Gamma_{0\to\infty}$ for typical junction parameters, one expects to see a large enhancement in the escape rate if a microwave source is used to resonantly excite the system from the ground state $|0\rangle$ to the first excited state $|1\rangle$ (see Fig. 3).[2]

Each microwave resonance in this system will be broadened due to the interaction of the junction with noise transmitted via the wiring which is described by the interaction

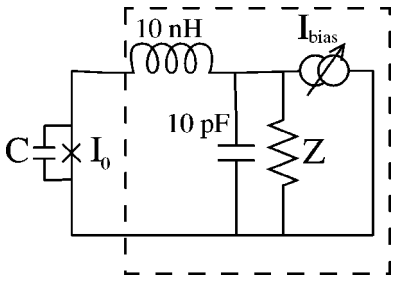

FIG. 1. Circuit schematic of current-biased Josephson junction connected to an LC isolation network and a current source. All the elements in the dashed box are represented by an equivalent resistance $R(\omega)$.

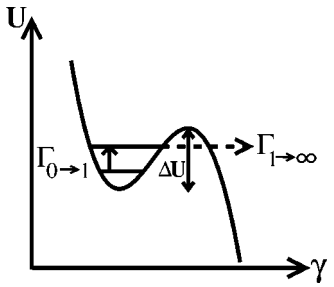

FIG. 2. Josephson-junction potential energy U as a function of the phase difference γ.

Hamiltonian $H_{int}=-(\Phi_0/2\pi)I_{noise}\gamma$. Thermal noise and dissipation at the transition frequencies will cause changes in the populations of the states. At low frequencies, the resonant terms are insignificant and the noise only causes dephasing.

Considering just the ground state $|0\rangle$ and the first excited state $|1\rangle$, transitions arise from thermal excitation from $|0\rangle$ to $|1\rangle$, a $1/RC$ decay rate from $|1\rangle$ to $|0\rangle$, and tunneling to the continuum, $\Gamma_{i\to\infty}$ for $i=0$ and 1. At temperature T, the combined transition rates from thermal and dissipative processes are[12]

$$\Gamma_{0\to 1}=\frac{1}{RC[\exp(\Delta E/kT)-1]}, \tag{2}$$

$$\Gamma_{1\to 0}=\frac{1}{RC[1-\exp(-\Delta E/kT)]}, \tag{3}$$

where $\Delta E=E_1-E_0$ is the difference in energy between the two levels. For $kT\ll\Delta E$, the upward transition rate is much smaller than the downward rate. Tunneling to the continuum is much smaller for the ground state than for the excited state in the anharmonic region of interest where $\Delta U/\hbar\omega\simeq 3$.[11] Thus, we expect that the full spectroscopic width of the $|0\rangle\to|1\rangle$ transition is

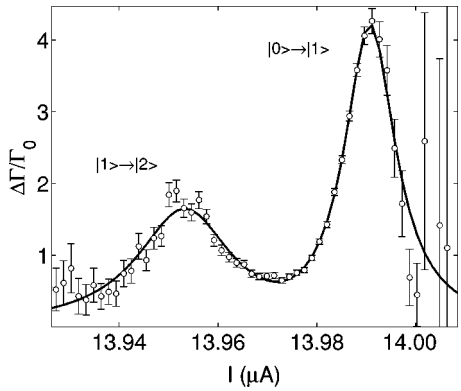

FIG. 3. Enhancement of escape rate under 5.7-GHz microwave drive. Left axis is the difference in escape rate with and without microwaves divided by the escape rate without microwaves. The large errorbars on the left and right of figure come from a lack of counts in the escape histogram. The right peak is $|0\rangle\to|1\rangle$ quantum transition, while left peak is $|1\rangle\to|2\rangle$. Solid line is a Lorentzian fit to two peaks.

$$\Delta\omega=\Gamma_{1\to\infty}+\Gamma_{0\to\infty}+\Gamma_{0\to 1}+\Gamma_{1\to 0}\simeq\Gamma_{1\to 0}+\Gamma_{1\to\infty}$$
$$\simeq 1/RC+\Gamma_{1\to\infty}. \tag{4}$$

Equations (1) and (4) imply that the level broadening, $\Delta\omega$, depends on bias through the $\Gamma_{1\to\infty}$ term and should exceed $1/RC$ as the bias current approaches I_0.

To understand results on real junctions, we must also take into account the dephasing effects of current noise in the system. For sufficiently low-frequency noise, we can model this nonresonant decoherence mechanism as a simple smearing of the response with bias. The resulting broadening of the spectroscopic width depends on how sensitive the resonant frequency ω is to changes in current, $\partial\omega/\partial I$; an rms current noise σ_I produces an additional contribution to the spectroscopic width of approximately $2\sigma_I\partial\omega/\partial I$. Including this current noise contribution in the previous form for the spectroscopic width gives

$$\Delta\omega\simeq 1/RC+\Gamma_{1\to\infty}+2\sigma_I\partial\omega/\partial I. \tag{5}$$

Both the second and the third terms in Eq. (5) depend on bias current, so that care must be taken in disentangling the two effects.

Using double angle evaporation, we fabricated 20 $\times 5\ \mu\mathrm{m})^2$ Al/AlOx/Al Josephson junctions with $J_c\simeq 14$ A/cm^2. Direct measurements of the junction current-voltage characteristics showed a subgap resistance of more than $10^4\ \Omega$ at 20 mK. Escape-rate measurements were made in an Oxford Instruments Model 200 dilution refrigerator with a 20 mK base temperature. We were able to tune the critical current of the junction by means of a superconducting magnet. The junctions were partially isolated from the bias leads by a 10 nH surface mount series inductor and a 10 pF capacitive shunt across the dissipative 50 Ω transmission line leads (see Fig. 1). This isolation scheme was designed so that at the plasma frequency, the effective shunt resistance due to the leads would be stepped up from 50 Ω to much more than $10^3\ \Omega$, increasing the intrinsic Q of the system. To perform escape-rate measurements, we start a timer and then ramp the current slowly (5 mA/s) using an HP 33120A function generator through a 47 kΩ resistor and monitor the junction voltage with a 2SK117 FET followed by an SRS560 amplifier. This output voltage is used to trigger the stop of timer, which is handled by a 20-MHz clock. Escape events were binned in time with width $t_w\simeq 50$ ns to create a histogram $H(t_i)$. The escape rate is then $\Gamma(t_j)=(1/t_w)\ln[\Sigma_{i=j}^{\infty}H(t_i)/\Sigma_{i=j+1}^{\infty}H(t_i)]$. We convert the time axis to current by calibrating the ramp current as a function of time.

We determine the spacing of the energy levels by comparing escape-rate curves with (Γ_m) and without (Γ_0) a small microwave drive current applied. Figure 3 shows $\Delta\Gamma/\Gamma_0=(\Gamma_m-\Gamma_0)/\Gamma_0$ for a 5.7-GHz microwave signal. We chose the power so that $\Delta\Gamma/\Gamma_0\lesssim 10$ on resonance to ensure the occupancy of $|1\rangle$ is small. Two Lorentzian peaks are apparent, corresponding to the $|0\rangle\to|1\rangle$ and $|1\rangle\to|2\rangle$ transitions. By measuring $\Delta\Gamma/\Gamma_0$ for different applied microwave frequency, we can measure how the bias current changes the energy-level spacing of the $|0\rangle\to|1\rangle$ transition [see Fig. 4(a)].

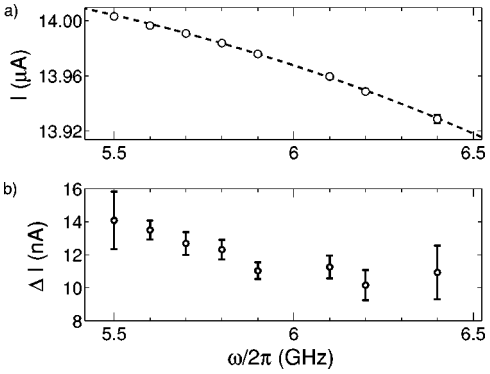

FIG. 4. (a) Drive frequency vs center of the $|0\rangle \rightarrow |1\rangle$ resonance peak for $I_0 = 14.12\ \mu$A. The dashed line is a fit to theory. (b) Full widths of each resonance for $I_0 = 14.12\ \mu$A. (Dataset No. 050902).

The data in Fig. 4(a) also allow us to compute $\partial\omega/\partial I$ and convert the full width at half maximum ΔI measured at each frequency [see Fig. 4(b)] to a width in frequency $\Delta\omega$ or the spectroscopic coherence time associated with the two levels, $\tau = 1/\Delta\omega$.

Figure 5 shows the coherence time τ as a function of the center current of each $|0\rangle \rightarrow |1\rangle$ peak. We note that the coherence time decreases markedly as I approaches $I_0 \simeq 14.12\ \mu$A, consistent with both escape-rate limiting of the lifetime of the upper state and excess low-frequency current noise, as in Eq. (5).

In principle, it is possible for the effective shunting impedance $R(\omega)$ to vary with frequency in such a way as to generate the changes in $\tau(\omega)$ seen in Fig. 5. We can rule out this explanation for the overall behavior of $\tau(\omega)$ by changing the critical current of the junction and remeasuring at the same frequency. Such a process changes $\Gamma_{i\rightarrow\infty}$ but not $R(\omega)$ in Eq. (5). Results for two different I_0's are plotted in Figs. 6(a) and 6(b). Comparison of Figs. 6(a) and 6(b) reveals that the coherence time at fixed frequency is lower for larger I_0. Since this measurement is at fixed frequency, the effect cannot be due to R varying with frequency. On the other hand, it is consistent with current noise and escape-rate lifetime limiting.

To distinguish the effects of current noise and escape-rate broadening in Eq. (5), we need to obtain an independent

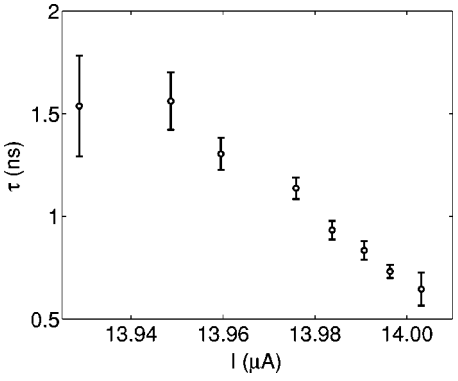

FIG. 5. Coherence time τ vs bias current I. Note that the escape rate from the ground state at 13.93 μA is around 10^3/s while at 14.01 μA, it is around 3×10^6/s.

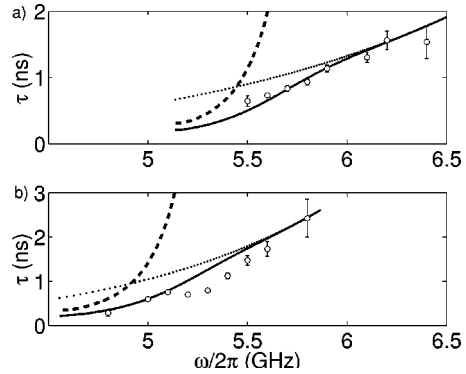

FIG. 6. Coherence time τ vs bias current I. Solid lines are the theoretical fit for each dataset. Lower frequency corresponds to larger current. The parameters for the fit in (a) are $I_0 = 14.12\ \mu$A and $C = 3.7$ pF. For the fit in (b) are $I_0 = 10.645\ \mu$A and $C = 3.7$ pF. The dashed lines represent the contribution from the escape rate and the dotted lines the contribution from current noise.

measure of the junction parameters. For the low critical current data, we fit the escape-rate curves without microwaves[13] and find $I_0 = 10.65 \pm 0.01\ \mu$A, $C = 3.7 \pm 0.3$ pF, and $T = 60 \pm 3$ mK. The 60 mK temperature was 40 mK above the base temperature, probably due to self-heating. We also numerically solved Schrödinger's equation (for the washboard potential with hard wall boundary conditions) and chose I_0 and C to fit the data in Fig. (4)(a) (dashed line). This yielded $I_0 = 10.66 \pm 0.07\ \mu$A and $C = 3.9 \pm 0.2$ pF. The same analysis for the high-I_0 case gives $I_0 = 14.143 \pm 0.003\ \mu$A and $C = 4.2 \pm 0.6$ pF.

We now fit the coherence time data in Fig. 6 by varying I_0 and C and comparing the results with the previously determined parameters. We find $\Gamma_{1\rightarrow\infty}$ by solving Schrödinger's equation numerically. To estimate the rms current noise σ_I, we note that the full current width at half maximum shown in Fig. 4(b) never drops below 10 nA. We thus assign $\sigma_I \simeq 5$ nA. To get a unique fit, we also assume $RC \gg 1/(2\sigma_I \partial\omega/\partial I)$. The solid lines in Fig. 6 show the results of this procedure. The dashed lines show the contribution to the broadening due to the escape rate alone, while the dotted lines represent the current noise contribution. The parameters for the lifetime fits, $I_0 = 14.12\ \mu$A, $C = 3.7$ pF, and $I_0 = 10.645\ \mu$A, $C = 3.7$ pF, agree with the parameters obtained from Fig. 4, verifying the inclusion of current noise and escape-rate-limited coherence in the model of Eq. (5). We note that as the bias current approaches I_0 (low frequency), the escape-rate term begins to dominate the lifetime, while for lower currents (high frequency), the noise broadening dominates.

If the junction qubit decoherence is dominated by current noise, the junction can be biased at low currents to reduce dephasing. To achieve N_{op} gate operations, each taking $N_g(2\pi/\omega)$ time, before decoherence occurs, requires the bias current be reduced to $I_{dc}/I_c < 2I_c/\sigma_I N_{op} N_g$. In principle, single junction gating schemes may allow such biasing at low currents where the junction is effectively decoupled from current noise. However, typical single junction gate operations require high bias currents to split the $|0\rangle \rightarrow |1\rangle$ tran-

sition from the $|1\rangle \rightarrow |2\rangle$ transition by at least the Rabi frequency of the $|0\rangle \rightarrow |1\rangle$ transition. Given that all junction systems will have some current noise, investigation of gating methods that work at low bias current would be interesting.

Finally, if low-frequency current noise is not a significant issue,[4] Eq. (1) leads to the requirement that the junction be biased such that there are $N_s > \frac{5}{36}\ln(N_{op}N_g) + \frac{5}{24}\ln(432N_s)$ levels in the well. For $N_{op} = 10^6$ and $N_g = 10$, we find $N_s > 4$.

To conclude, we have measured the resonance width of the transition between the lowest two quantum states in a Josephson-junction qubit as a function of bias current, and found that the lifetime of the excited state falls rapidly as the bias current I approaches I_0. A model including continuous dephasing from tunneling as well as from current noise explains quantitatively the reduced coherence time. This ability to predict and calculate such junction behavior is crucial to the use of junctions in quantum computers and is one of the reasons that junctions are a good candidate qubit.

We acknowledge support from DOD and the Center for Superconductivity Research and thank A. J. Dragt, P. R. Johnson, J. M. Martinis, F. W. Strauch, and R. A. Webb for many useful discussions.

*Electronic address: berkley@physics.umd.edu

[1] R.F. Voss and R.A. Webb, Phys. Rev. Lett. **47**, 265 (1981).

[2] J.M. Martinis, M.H. Devoret, and J. Clarke, Phys. Rev. Lett. **55**, 1543 (1985).

[3] R.C. Ramos, M.A. Gubrud, A.J. Berkley, J.R. Anderson, C.J. Lobb, and F.C. Wellstood, IEEE Trans. Appl. Supercond. **11**, 998 (2001).

[4] J.M. Martinis, S. Nam, J. Aumentado, and C. Urbina, Phys. Rev. Lett. **89**, 117901 (2002).

[5] A. Blais, A. Maassen van den Brink, and A.M. Zagoskin, Phys. Rev. Lett. **90**, 127901 (2003).

[6] F.W. Strauch *et al.*, quant-ph/0303002 (unpublished).

[7] A.J. Berkley *et al.*, Science **300**, 1548 (2003).

[8] Y. Yu, S. Han, X. Chu, S. Chu, and Z. Wang, Science **296**, 886 (2002).

[9] J.M. Martinis, S. Nam, J. Aumentado, K.M. Lang, and C. Urbina, Phys. Rev. B **67**, 094510 (2003).

[10] See, e.g., M. Tinkham, *Introduction to Superconductivity*, 2nd ed. (McGraw Hill, New York, 1996).

[11] G. Alvarez, Phys. Rev. A **37**, 4079 (1988).

[12] K.S. Chow, D.A. Browne, and V. Ambegaokar, Phys. Rev. B **37**, 1624 (1988).

[13] M. Büttiker, E.P. Harris, and R. Landauer, Phys. Rev. B **28**, 1268 (1983).